Final Report (DE-FG02-01ER15120 (1999-2008)

The original funding under this project number was awarded for a period 12/1999 until 12/2002 under the project title *Diamond and Hydrogenated Carbons for Advanced Batteries and Fuel Cells: Fundamental Studies and Applications*. The project was extended until 06/2003 at which time a renewal proposal was awarded for a period 06/2003 until 06/2008 under the project title *Metal/Diamond Composite Thin-Film Electrodes: New Carbon Supported Catalytic Electrodes*. The work under DE-FG02-01ER15120 was initiated about the time the PI moved his research group from the Department of Chemistry at Utah State University to the Department of Chemistry at Michigan State University. This DOE-funded research was focused on (i) understanding structure-function relationships at boron-doped diamond thin-film electrodes, (ii) understanding metal phase formation on diamond thin films and developing electrochemical approaches for producing highly dispersed electrocatalyst particles (e.g., Pt) of small nominal particle size, (iii) studying the electrochemical activity of the electrocatalytic electrodes for hydrogen oxidation and oxygen reduction and (iv) conducting the initial synthesis of high surface area diamond powders and evaluating their electrical and electrochemical properties when mixed with a Teflon binder. (Note: All potentials are reported versus Ag/AgCl (sat'd KCl) and cm^2 refers to the electrode geometric area, unless otherwise stated).

1. *The Effect of sp^2-Bonded Nondiamond Carbon Impurity on the Physical and Electrochemical Properties of Boron-doped Polycrystalline Diamond Thin-Film Electrodes* (*J. Electrochem. Soc.* **2004**, 151, E306). Even though the diamond electrode has been used in electrochemistry for over ten years now, there is still a great deal unknown about the factors that affect its electrochemical activity with several being important including (i) the dopant type and level, (ii) surface chemistry, (iii) morphology and microstructure and (iv) the nondiamond carbon impurity content. The effect of the latter was investigated and reported on. The physical and electrochemical properties of boron-doped polycrystalline diamond thin-film electrode, prepared with varying levels of sp^2-bonded nondiamond carbon impurity, were systematically investigated. This impurity was introduced through adjustment of the methane-to-hydrogen (C/H) source gas ratio used for the deposition from 0.3 to 5% (v/v). Proportional increases in the fraction of grain boundary, the extent of secondary crystallite growth, and the amount of sp^2-bonded carbon impurity resulted with increasing C/H ratio. Variations in the morphology and microstructure were monitored using atomic force microscopy (AFM) and Raman spectroscopy, respectively. The electrode response was assessed, using $Fe(CN)_6^{3-/4-}$, $Ru(NH_3)_6^{3+/2+}$, $Fe^{3+/2+}$, and 4-*tert*-butylcatechol (4-tBC). All were 1 mM in concentration and mixed with either 1 M KCl or 0.1 M $HClO_4$. While the increased sp^2-bonded carbon content had little effect on the cyclic voltammetric peak separation (ΔE_p) and peak current for the first two redox systems, the impurity had a significant impact on the latter two, as ΔE_p decreased proportionally with the increasing sp^2-bonded carbon content. The effect of the impurity on the reduction of oxygen in 0.1 M $HClO_4$ and 0.1 M NaOH was also investigated. A direct correlation was found between the impurity level, as estimated from Raman spectroscopy, and the overpotential for oxygen reduction. The greater the nondiamond content, the lower the kinetic overpotential for the reduction reaction. Tafel plots yielded an apparent exchange current density that increased and a transfer coefficient that decreased with increasing nondiamond carbon content. *The results demonstrate that the grain boundaries, and the sp^2 carbon impurity presumably residing there, can have a significant impact on the electrode reaction kinetics for certain redox systems, and little influence for others.* Understanding the influence of the nondiamond carbon is important for the diamond powder electrode development (*vide infra*) because its controlled incorporation may be a way to impart a greater degree of activity for the oxygen reduction reaction to the carbon.

2. *The Electrochemical Performance of Diamond Thin-Film Electrodes from Different Commercial Sources* (*Anal. Chem.* **2004,** 76, 2553). The diamond electrode is finding more and more use in present day electrochemistry, in part, because it is commercially available from several sources. With any new electrode, especially carbon, it is important to verify that the material available possesses the expected electrochemical properties and that these properties are reproducible from source to source. To this end, the electrochemical properties of two commercial (Condias and Sumitomo) boron-doped diamond thin-film electrodes were compared

with the properties of two boron-doped diamond thin-film types deposited in our laboratory (so-called microcrystalline and nanocrystalline). Scanning electron microscopy (SEM) and Raman spectroscopy were used to characterize the electrode morphology and microstructure, respectively. Cyclic voltammetry was used to study the electrochemical response toward five different redox systems: $Fe(CN)_6^{3-/4-}$, $Ru(NH_3)_6^{3+/2+}$, $IrCl_6^{2-/3-}$, 4-methylcatechol, and $Fe^{3+/2+}$. *The response was found to be reproducible from electrode type-to-type for all the redox systems.* For all five, the forward reaction peak current varied linearly with the scan rate$^{1/2}$ (ν), indicative of electrode reaction kinetics controlled by mass transport (semi-infinite linear diffusion) of the reactant. Apparent heterogeneous electron-transfer rate constants, k°_{app}, for all five redox systems were determined from ΔE_p-ν experimental data, according to the method described by Nicholson (). The rate constants were also verified through digital simulation (DigiSim® 3.03) of the voltammetric i-E curves at different scan rates. Good fits between the experimental and simulated voltammograms were found for scan rates up to 50 V/s. k°_{app} values of 0.05 to 0.5 cm/s were observed for $Fe(CN)_6^{3-/4-}$, $Ru(NH_3)_6^{3+/2+}$, and $IrCl_6^{2-/3-}$ without any conventional electrode pretreatment (e.g., polishing). Lower k°_{app} values of 10^{-4} to 10^{-6} cm/s were found for 4-methylcatechol and $Fe^{3+/2+}$. The voltammetric responses for $Fe(CN)_6^{3-/4-}$ and $Ru(NH_3)_6^{3+/2+}$ were also examined for all four electrode types at two different solution pH (1.90 and 7.35). Since the hydrogen-terminated diamond surfaces contain few, if any, ionizable carbon-oxygen functionalities (e.g., carboxylic acid, pK_a ~4.5), the ΔE_p, i_p^{ox} and i_p^{red} values for the two systems were, for the most part, unaffected by the solution pH. This is in contrast to the typical behavior of oxygenated, sp^2 carbon electrodes, such as glassy carbon (51).

3. *Scanning Electrochemical Microscopy (SECM) and Conductive Probe Atomic Force Microscopy (CP-AFM) Studies of Hydrogen-Terminated Boron-Doped Diamond Electrodes With Different Doping Levels.* (*J. Phys. Chem. B* **2004**, 108, 15117). Collaboratively with the Bard group, we began to investigate the homogeneity of the electrical conductivity and electrochemical activity across boron-doped microcrystalline diamond thin-film electrode surfaces using conductivity probe-atomic force microscopy (CP-AFM) and scanning electrochemical microscopy (SECM). The pattern of conductivity and electrochemical activity for hydrogen-terminated boron-doped diamond electrodes with different doping levels were measured. CP–AFM showed the surface was predominantly of low conductivity, with discrete conducting areas less than 2 μm in diameter, randomly and non-uniformly distributed over the surface. SECM imaging correlated these conductive areas with electrochemical activity, and showed that the electrode surface was only partially active and that the active area increased with boron doping level. Cyclic voltammograms and SECM approach curves, obtained for $Ru(NH_3)_6^{3+/2+}$, were characteristic of those obtained at a partially blocked electrode of non-uniform activity, or a microelectrode array. Using this model, SECM approach curves could be fit to obtain values of the fraction of the surface that was electrochemically active. These two techniques are presently being used in our laboratory for electrode characterization. Figure 2 shows typical CP-AFM (left) and SECM current images (right) for $Ru(NH_3)_6^{+3/+2}$ at a highly boron-doped nanocrystalline diamond thin-film electrode. The CP-AFM image was acquired using a bias

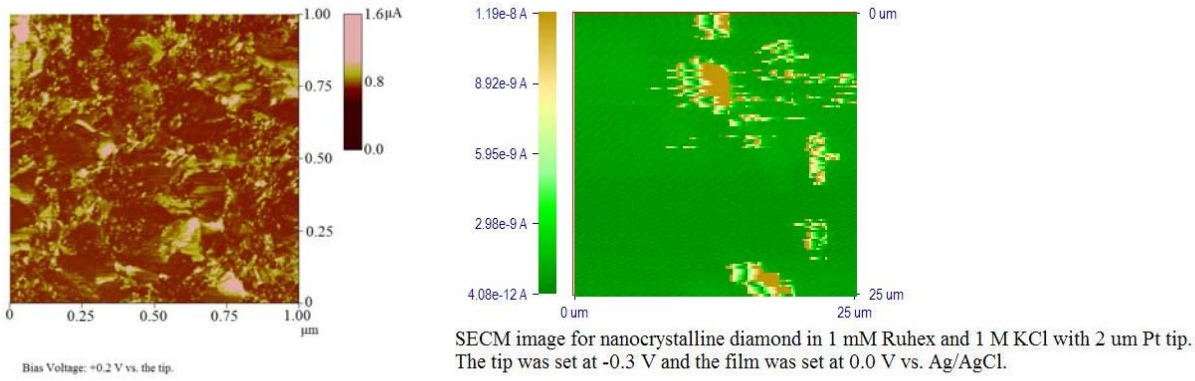

SECM image for nanocrystalline diamond in 1 mM Ruhex and 1 M KCl with 2 um Pt tip. The tip was set at -0.3 V and the film was set at 0.0 V vs. Ag/AgCl.

Figure 2. CP-AFM image (left) and an SECM image for $Ru(NH_3)_6^{+3/+2}$ at a boron-doped nanocrystalline diamond electrode.

voltage of 0.2 V. The heterogeneous nature of the electrical conductivity across the surface is clearly revealed. Highly conducting areas (bright) are separated from one another by less conducting (dark) regions. The SECM image was obtained in the *tip generation-substrate collection mode*. The tip potential was -0.3 V (diffusion limited reduction of $Ru(NH_3)_6^{+3}$) and the diamond electrode potential was 0 V (diffusion limited oxidation of $Ru(NH_3)_6^{+2}$). The bright areas are associated with the regions of highest electrochemical activity. The surface clearly possesses heterogeneous electrochemical activity toward this redox system. We are presently using these tools to study the properties of the electrode materials and seek to gain more insight as to why these heterogeneities exist. The heterogeneous nature does not preclude its use as electrode material, but rather explains some of its properties. Similar heterogeneous activity has been observed for other solid carbon electrodes (e.g., glassy carbon).

4. *Pulsed Galvanostatic Deposition of Pt Particles on Microcrystalline and Nanocrystalline Diamond Thin-Film Electrodes. Part I: Characterization of As-Deposited Metal/Diamond Surfaces*. (*J. Electrochem. Soc.* **2005**, 152, E184). In previous work, we prepared and characterized metal/diamond composite electrodes (11-13). These highly stable and corrosion resistant electrodes were formed by electrodepositing (DC potential) Pt metal on a diamond film surface and then anchoring the particles within a thin secondary diamond layer. These electrodes possessed excellent dimensional stability even during exposure to strongly oxidizing conditions, but the metal particle size was too large (150-300 nm) and the dispersity too low for practical use. Pulsed galvanostatic deposition was subsequently investigated to learn how effective it can be for forming small diameter and highly dispersed Pt particles on electrically conducting microcrystalline and nanocrystalline diamond thin-film electrodes. The deposition was studied as a function of pulse number (10 to 50) and current density (0.50 to 1.50 mA cm^{-2}) at the two morphologically different forms of diamond. The deposition of catalyst particles using ten 1-s pulses (duty cycle 50%) at a current density of 1.25 mA cm^{-2} (geometric area) produced the smallest nominal particle size and the highest particle coverage on both diamond surfaces. Secondary electron micrographs (SEM) revealed metal coverage over all the surface (contrary to the SECM data), a nominal particle size of 43 ± 27 nm (RSD = 63%) for microcrystalline and 25 ± 25 nm (RSD = 100%) for nanocrystalline diamond, and a nominal particle coverage of 7.5 (± 0.9) x 10^9 cm^{-2} for microcrystalline and 1.9 (± 1.0) x 10^{10} cm^{-2} for nanocrystalline diamond. Deposition under these conditions produced the highest catalytic activity for hydrogen adsorption/ desorption and oxygen reduction, based on the electrochemically-active Pt area normalized to the estimated metal loading. Typical specific surface areas of 10-50 m^2/g_{Pt} were calculated, which compare favorably to values obtained for sp^2 electrodes, like carbon and graphite. The influence of the microstructure and electronic properties on the formation of dimensionally uniform metal adlayers was discussed.

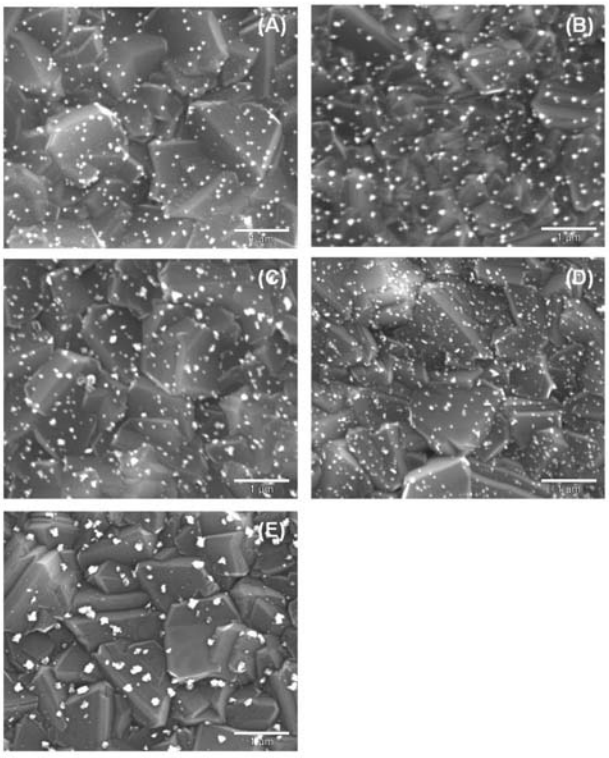

Figure 3. SEM images of microcrystalline diamond thin-film electrodes decorated with Pt metal particles using pulsed galvanostatic deposition at current densities from 0.05 to 1.50 mA/cm^2.

SEM images of the Pt adlayers formed on microcrystalline diamond as a function of the pulse current density from 0.50 to 1.50 mA/cm^2 (geometric area) are presented in Figure 3A-E. The deposition was carried out using a pulse number of 10 and a pulse width of 1 s. Table 1 presents a summary of the particle analysis data. Statistically, the nominal particle size was the same for all five current densities, ranging from 40-70 nm with an RSD of approximately 50%.

The particle coverage increased from 1.3 ($\pm$ 1.0) to 7.5 ($\pm$ 0.9) x 10^9 cm^{-2} with current density up to 1.25 mA/cm^2. For the highest current density though, 1.50 mA/cm^2, the particle coverage decreased to 1.9 ($\pm$ 0.9) x 10^9 cm^2. The film deposited at 1.25 mA/cm^2 had particles that were nominally the same size as those produced at 0.50 mA/cm^2, but with a particle density nearly 6 times greater. It was concluded that this is a viable deposition method for producing relatively small and highly dispersed metal deposits on diamond, although some refinement is still needed to reduce the particle size to the 5-10 nm range and to further control the particle morphology (8-10). We also reported on the effect of the secondary diamond growth on the stability and activity of the electrocatalyst. We will endeavor to use this method to impregnate the high surface area diamond and modified *sp*^{2} carbon support materials (*vide infra*).

Table 1. Particle Analysis and Hydrogen Adsorption Data for Pt-Coated Microcrystalline Diamond Films as a Function of the Pulse Current Density

Pulse Current Density (mA/cm^2)[a]	Mean Particle Size (nm)	Particle Coverage (cm^{-2})[a]	Hydrogen Adsorption Charge (mC/cm^2)[a]
0.50	46 $\pm$ 27	1.3 ($\pm$ 1.0) x 10^9	0.066 $\pm$ 0.014
0.75	65 $\pm$ 37	1.5 ($\pm$ 0.4) x 10^9	0.095 $\pm$ 0.005
1.00	59 $\pm$ 34	2.2 ($\pm$ 0.6) x 10^9	0.11 $\pm$ 0.01
1.25	43 $\pm$ 27	7.5 ($\pm$ 0.9) x 10^9	0.16 $\pm$ 0.01
1.50	68 $\pm$ 43	1.9 ($\pm$ 0.9) x 10^9	0.19 $\pm$ 0.03

5. ***Studies of the Oxygen Reduction Reaction at Electrocatalytic Pt/Diamond Electrodes*** (manuscript in preparation). The oxygen reduction reaction was investigated in 0.1 M $HClO_4$ at the two types of diamond modified with nanometer-sized Pt electrocatalyst particles. The pulsed galvanostatic deposition method was used to modify microcrystalline and nanocrystalline diamond thin-film electrodes with Pt adlayers. We sought to investigate the degree of electronic coupling between the metal and the diamond support, as well as the effectiveness of the electrocatalytic electrode for the oxygen reduction reaction. With increasing pulse number and pulse current density, a positive shift in the voltammetric reduction peak potential (E_p^{red}) and an increase in the peak current were seen. This is consistent with an increase in the catalytic activity of the electrode. E_p^{red} for both electrodes was ca. 410 mV vs. Ag/AgCl. Tafel slopes of -75 $\pm$ 1.8 and -68 $\pm$ 1.9 mV/dec were observed for the Pt/microdiamond and Pt/nanodiamond electrodes; both prepared with ten 1-s pulses at 1.25 mA/cm^2. These films possessed particles with the most optimal properties in terms of particle size and density. Similar slopes were observed for polycrystalline Pt as well as Pt deposited on a model sp^2-bonded carbon electrode, glassy carbon, using the same deposition conditions. More detailed investigation of the oxygen reduction reaction at Pt/diamond electrodes is currently ongoing.

In summary, we have learned a great deal about metal phase formation on diamond, the stability and electrocatalytic activity of the metal/diamond electrodes, some of the factors that

influence the electrochemical properties of this new electrode material and the heterogeneity of the electrical and electrochemical properties across a polycrystalline film surface. All of this work was performed with planar thin-film electrodes. Obviously, these electrodes do not possess the surface area or gas permeability needed for fuel cell application. Therefore, research was begun on the synthesis of higher surface area forms of electrically conducting diamond. This will continue to be a major focus in the proposed proposed. Below, some of the preliminary results for the synthesis and characterization of higher surface area diamond are described.

6. Preparation and Characterization of Boron-Doped Diamond Powder: A Possible Dimensionally Stable Electrocatalyst Support Material. (*J. Electrochem. Soc.* **2005**, 152, B369). Our past work has indicated that diamond possesses superb dimensional stability and corrosion resistance even during exposure to strongly oxidizing conditions (11-13,15,46,47). All of this work used thin-film electrodes that are impractical for fuel cell applications due to a low surface area and impermeability to gases. If diamond is to become a viable electrocatalyst support material, it will have to be available in a high surface area form. The thin-film electrode is available for relatively low cost but higher surface area forms are not. Efforts to synthesize conducting diamond in a higher surface area form began by simply coating inexpensive insulating diamond powder with an overlayer of boron-doped diamond. The preparation, characterization and evaluation of the electrochemical properties of electrically conducting diamond powder was described.

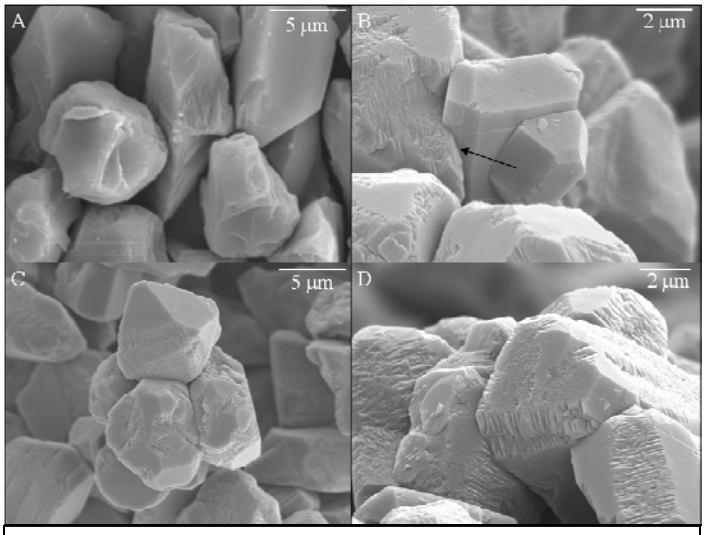

Figure 4. SEM images of diamond powders (A) before, and (B-D) after conductive diamond deposition for 1, 2 and 6-h depositions.

The conducting powder was prepared by coating insulating diamond powder (8-12 μm diam, ~2 m^2/g) with a thin boron-doped overlayer using microwave plasma-assisted chemical vapor deposition. Deposition times from 1 to 6 h were evaluated. The surface area of this powder (~2 m^2/g) is lower than that desired for an ideal support (100 m^2/g) but, nevertheless, is a useful starting point for making a conductive powder and evaluating its physical, electrical, and electrochemical properties. *We still have much to learn about making electrodes with this new material in terms of optimizing the particle contact, amount of binder used, thickness and preparing MEAs. The numerical simulations outlined below will help to direct the optimization process.* SEM revealed that the diamond powder particles become more faceted and more secondary growths form with increasing deposition time. This can be seen in the SEM images presented in Figure 4A-D. Although it is difficult to distinguish differences in particle size, changes in the powder morphology are apparent with increasing deposition time. The uncoated powder particles in Figure 4A are irregularly shaped and characterized by jagged edges having little faceting. Figure 4B shows a powder sample after a 1-h deposition. The particle edges become smoother and more faceting develops. Many of the particle surfaces consist of multiple grooves along the edges of the triangular facets. There are also some pits present on the facets. These grooves may be sites of preferential nucleation. It is possible that carbon atoms nucleate at these defect sites and growth occurs laterally across the surface. The pits on the facet surface may result from incomplete coalescence of growth layers across the surface, which begin at different nucleation sites. The most obvious morphological change after diamond deposition is the fusion of neighboring particles, as indicated by the arrow in Figure 4B. After the 2-h deposition, neighboring particles continue to fuse together forming clusters of 4 or 5 grains, as seen in Figure

4C. These clusters become larger with increasing deposition time. Clusters of 8 to 10 particles formed after the 4-h deposition and even larger clusters formed after the 6-h period (see Fig. 4D). While this particle fusion reduces the surface area to some extent, it is actually beneficial in terms of increasing the electrical conductivity of the material (i.e., increased carrier mobility).

The first-order diamond phonon line appeared in the Raman spectrum at ca. 1331 cm^{-1} for deposition times up to 4 h, and was downshifted to as low as 1317 cm^{-1} for some particles after the 6-h growth. Electrical resistance measurements of the bulk powder (no binder) confirmed that a conductive diamond overlayer formed, as the conductivity increased from near zero (insulating, < 10^{-5} S/cm) for the uncoated powder to 1.5 S/cm after the 6-h growth. Ohmic behavior was seen in current-voltage curves recorded for the 4-h powder between ± 10 V. Cyclic voltammetric *i-E* curves for $Fe(CN)_6^{3-/4-}$ and $Ru(NH_3)_6^{3+/2+}$ were recorded to evaluate the electrochemical properties of the conductive powder when mixed with a polytetrafluoroethylene binder (10 wt. %). At scan rates between 10 and 500 mV/s, ΔE_p for both redox systems was high ranging from 140 to 350 mV, consistent with significant ohmic resistance within the powder/binder electrode. Results suggested that the resistance is mainly due to poor particle-particle connectivity because of the amount of binder used to prepare the electrode. For example, reducing the amount of binder from 10 to 5% resulted in a significant reduction in the ΔE_p for these two redox systems to < 100 mV. Potentiostatic polarization at 1.6 V vs. Ag/AgCl for 1 h (25 ºC) was performed to evaluate the morphological and microstructural stability of the conductive diamond in comparison with graphite and glassy carbon (GC) powders. The total charge passed during polarization was largest for the GC powder (0.88 C/cm^2) and smallest for conductive diamond powder (0.18 C/cm^2). SEM images taken of the conductive diamond powder after polarization showed no evidence of any microstructural degradation while significant morphological and microstructural damage were seen for the GC powder. *The preparation of higher surface area and more conducting diamond powders, as well as their formation, into useful electrodes will be a focal point of the research proposed herein.*

7. *Preparation and Characterization of Boron-Doped Diamond Paper with Pt Nanoparticles*. (*J. Electrochem. Soc.*, **2007**, 154, K61). A procedure was developed for modifying the surface of Toray carbon paper (TCP – a diffusion layer material) with a layer of boron-doped nanocrystalline diamond. The application of a hydrophobic surface coating could prove useful for improved water management in the diffusion layer. The diamond was deposited via microwave-assisted plasma CVD. SEM revealed that fibers within the first ~100 μm of the TCP structure were fully coated with nanocrystalline diamond (film thickness ~1 μm). XRD and Raman spectroscopy confirmed that the TCP was coated with a crystalline diamond overlayer. The SEM images in Figure 5 show (A) the uncoated fiber mesh, (B) striations on the individual carbon fibers prior to diamond deposition, (C) the nanocrystalline morphology of the diamond overlayer and (D) a cross-sectional view of a coated carbon fiber.

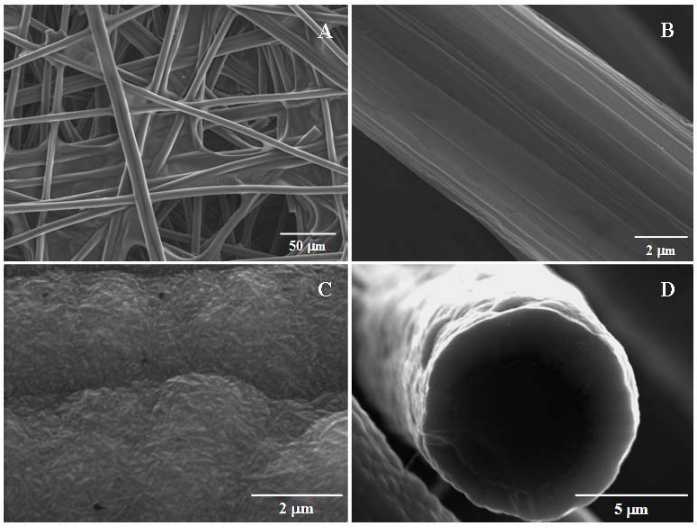

Figure 5. SEM images of the uncoated and diamond-coated Toray paper.

The microstructural stability of the TCP and the diamond-coated TCP, with and without Pt electrocatalyst, was evaluated after

potentiostatic polarization at 1.4 and 1.6 V vs. Ag/AgCl for 1 h at 25 ºC. The supporting electrolyte was 0.1 M $HClO_4$. Polarizations could not be conducted at 80 ºC because the insulating material (nail polish) was unstable in acid at this high temperature. No morphological or microstructural alterations were seen for either the coated or uncoated TCP after polarization at 1.4 V. However, severe degradation was observed for TCP after polarization at 1.6 V as the individual carbon fibers fractured and separated from the electrode. In contrast, no morphological damage was seen for the diamond-coated TCP. The degradation of TCP was even more pronounced at 1.6 V when Pt was present. Again though, no damage was seen for the Pt-containing diamond-coated TCP.

Preliminary investigation of the formation of Pt electrocatalyst layers on the diamond-coated TCP was carried out. Two different pulsed galvanostatic conditions (designated A and B) were used to electrodeposit Pt on bare (TCP) and diamond-coated TCP (BND). For A (0.146 mA/cm^2 or 0.0047 C/cm^2), large particles of low dispersity were formed on TCP, while nanoparticles with a large diameter of 177 ± 39 nm and a density of ~1.2 x 10^9 particles/cm^2 were formed on BND. For B (1.25 mA/cm^2 or 0.040 C/cm^2), Pt nanoparticles were deposited on both TCP (233 ± 89 nm diameter and ~2.7 x 10^8 particles/cm^2) and BND. The particles on BND, however, were so dense and closely spaced that an accurate measure of the particle size and density was impossible. The metal-containing carbon electrodes had surface enhancement factors (SEF, Pt surface area/electrode surface area) of 0.033, 0.50, 3.3, and 1.7 for Pt/TCP-A, Pt/BND-A, Pt/TCP-B, and Pt/BND-B, respectively. The specific Pt surface areas (S_{Pt}, m^2/g_{Pt}) were 1.4, 21, 16 and 8.2 for Pt/TCP-A, Pt/BND-A, Pt/TCP-B, and Pt/BND-B, respectively. The oxygen reduction reaction was used to probe the electrocatalytic activity of the composite electrodes. The most active electrode was Pt/BND-A with a half-wave potential, $E_{p/2}$, of 0.583 V vs. Ag/AgCl and a limiting current of ca. -1000 μA/SEF. *Clearly, more work is needed to optimize the formation of the electrocatalyst layer, but these preliminary results suggest that the electrocatalyst can be formed on the modified carbon paper and that electrocatalyst is active for the oxygen reduction reaction.*

Publication List

1. J. Wang, G. M. Swain, T. Tachibana and K. Kobashi, "Incorporation of Pt Particles in Boron-Doped Diamond Thin-Films: Applications in Electrocatalysis", *Electrochem. Solid-State Lett.*, **2000**, 3, 286.
2. J. Wang and G. M. Swain, "Dimensionally State Pt/Diamond Composite Electrodes in Concentrated H3PO4 at High Temperature", *Electrochem. Solid-State Lett.* **2002**, 5, E4.
3. J. Wang and G. M. Swain, "Fabrication and Evaluation of Platinum/Diamond Composite Electrodes for Electrocatalysis", *J. Electrochem. Soc.* **2003**, 150, E24.
3. J. A. Bennett, J. Wang, Y. Show, and G. M. Swain, "Effect of sp^2-Bonded Nondiamond Carbon Impurity on the response of Boron-Doped Polycrystalline Diamond Thin-Film Electrodes", *J. Electrochem. Soc*., **2004**, 151, E306.
4. K. B. Holt, A. J. Bard, Y. Show and G. M. Swain, "Scanning Electrochemical Microscopy and Conductive Probe Atomic Force Microscopy Studies of Hydrogen-Terminated Boron-Doped Diamond Electrodes with Different Doping Levels", *J. Phys. Chem.*, **2004**, 108, 15117.
5. A. E. Fischer, Y. Show, and G. M. Swain, "Electrochemical Performance of Diamond Thin-Film Electrodes from Different Commercial Sources", Anal. Chem., **2004**, 76, 2553.
6. J. A. Bennett, Y. Show and G. M. Swain, "Pulsed Galvanostatic Deposition of Pt Particles on Microcrystalline and Nanocrystalline Diamond Thin-Film Electrodes", *J. Electrochem. Soc*., **2005**, 152, E184.
7. A. E. Fischer and G. M. Swain, "Preparation and Characterization of Boron-Doped Diamond Powder: A Possible Dimensionally Stable Electrocatalyst Support Material", *J. Electrochem. Soc*. **2005**, 152, B359.
8. V. S. Robinson, T. S. Fisher, Y. Show, G. M. Swain, F. Pfefferkorn, "Thermionic Emission from Surface Terminated Nanocrystalline Diamond", *Diam. Rel. Mater.*, **2006**, 15, 1601.

9. M. A. Lowe, A. E. Fischer and G. M. Swain, "Deposition of Defect- and Stress-Free Boron-Doped Diamond Thin Film on Titanium Using a Dual Coating Strategy", *J. Electrochem. Soc.* **2006**, 153, B506.
10. S. Wang and G. M. Swain, "Spatial Heterogeneity of the Electrical and Electrochemical Properties of Hydrogen-Terminated Boron-Doped Nanocrystalline Diamond Thin Film Deposited from an Argon-Rich $CH_4/H_2/Ar/B_2H_6$ Source Gas Mixture", *J. Phys. Chem. C.* **2007**, 111, 3986.
11. V. M. Swope, I. Sasaki, A. Ay, and G. M. Swain, **"**Conductive diamond powder: a new catalyst support for the polymer electrolyte membrane fuel cell", *ECS Transactions*, **2007**, 3(28, Multifunctional Carbon Materials for Electrochemical and Electronic Applications), 27-36.
12. A. E. Fischer, M. A. Lowe, and G. M. Swain, **"**Preparation and Electrochemical Characterization of Carbon Paper Modified with a Layer of Boron-Doped Nanocrystalline Diamond," *J. Electrochem. Soc.*, **2007**, 154, K61.
13. A. Ay, V. M. Swope and G. M. Swain, "The Physicochemical and Electrochemical Properties of 100 and 500 nm Diameter Boron-Doped Diamond Powders Coated with Boron-Doped Nanocrystalline Diamond", *J. Electrochem. Soc.* **2008**, 155, B1013.
14. S. Wang, J. E. Butler and G. M. Swain, "The Structural and Electrochemical Properties of Boron-Doped Nanocrystalline Diamond Thin-Film Electrodes Grown from Ar-Rich and H_2-Rich Source Gases," *Diam. Rel. Mater*., **2009**, 18, 669.

Three additional manuscripts are presently in review with *Chemistry of Materials*, *J. Electrochem. Soc.*, and *Diam. Rel. Mater.*

Book Chapters

1. D. Knigge, P. Kaur and G. M. Swain, "Recent Trends in the Chemical Modification of sp^2 and sp^3 Bonded Carbon Electrodes" in Encyclopedia of Electrochemistry, Vol. 10. (Modified Electrodes), M. Fujihira, I. Rubinstein and J. F. Rusling, eds.; Wiley-VCH Verlag GmbH& Co., **2007**, pp 236-260.
2. Greg M. Swain "Chapter 5 - Solid Electrode Materials: Pretreatment and Activation", in Handbook of Electrochemistry, C. Zoski, ed.; Elsevier., **2007**, Chap.5; pp 111-153.

Patents

1. U.S. 6,884,290 B2. *Electrically Conductive Polycrystalline Diamond and Particulate Metal Based Electrodes*, G. M. Swain and J. Wang.
2. U.S. 7,144,753 B2. *Boron-Doped Nanocrystalline Diamond*, G. M. Swain, Y. Show, P. Sonthalia and M. Witek. [This patent covers the growth and electrochemical applications of boron-doped nanocrystalline diamond thin-film materials grown from Ar-rich source gas mixtures.]
3. G. M. Swain, A. Fischer, J. Bennett and M. Lowe, "Electrically Conductive Diamond Electrodes", U.S. Patent Appl. 11/378,109. (revised original application based on initial review in spring 2008, pending).